

Experimental Evaluation of Magnetic Vehicle Detection Using Low-cost LIS3MDL Microelectromechanical Systems Magnetometer

Nguyen Van Nghiem^{*†}

Hanoi 100000, Vietnam

(Received January 8, 2026; accepted March 13, 2026)

Keywords: magnetic sensing, MEMS magnetometer, vehicle detection, signal processing, geomagnetic disturbance

Magnetic sensing has been widely investigated for detecting ferromagnetic objects in outdoor environments and is commonly used in traffic monitoring and intelligent transportation applications. Low-cost microelectromechanical systems (MEMS) magnetometers provide an attractive sensing solution owing to their compact size, low power consumption, and ease of integration into embedded platforms. However, measurements obtained from such sensors are often affected by noise, baseline drift, and slowly varying geomagnetic disturbances, which may degrade vehicle detection reliability. In this paper, an experimental evaluation of magnetic vehicle detection using a low-cost LIS3MDL triaxial MEMS magnetometer is presented. A lightweight signal processing method based on moving-average baseline compensation is applied to suppress slowly varying geomagnetic variations while preserving transient disturbances generated by passing vehicles. Roadside experiments were conducted at a sampling frequency of 200 Hz. The results show that the proposed processing method improves measurement stability and increases the signal-to-noise ratio by more than 11 dB. Repeated experiments demonstrate reliable vehicle detection with a rate exceeding 96%.

1. Introduction

Magnetic sensing has become an important technique for detecting ferromagnetic objects in a wide range of applications, including traffic monitoring, intelligent transportation systems, industrial inspection, and infrastructure safety.^(1,2) Compared with optical or radar-based sensing technologies, magnetic sensors operate independently of lighting conditions and are largely insensitive to weather variations or visual occlusions. These characteristics make magnetic sensing particularly suitable for outdoor monitoring applications where robustness and low power consumption are essential.

Recent advances in microelectromechanical systems (MEMS) technology have enabled the development of compact and low-cost triaxial magnetometers.⁽³⁾ Devices such as the LIS3MDL

*Corresponding author: e-mail: nghiemmsc@gmail.com

†Independent researcher

<https://doi.org/10.18494/SAM6170>

triaxial MEMS magnetometer (STMicroelectronics, Geneva, Switzerland) provide digital measurements of the magnetic field along three orthogonal axes while maintaining low power consumption and simple hardware integration. As a result, MEMS magnetometers are increasingly employed in embedded sensing platforms, IoT devices, and distributed monitoring systems.^(4–6)

In vehicle detection scenarios, the presence of a vehicle disturbs the ambient geomagnetic field owing to the ferromagnetic materials contained in the vehicle body, engine, and chassis. These materials distort the surrounding magnetic flux distribution when exposed to the Earth's magnetic field.^(1,7) As the vehicle moves relative to a nearby sensor, a transient magnetic anomaly that can be detected using a magnetometer deployed near the roadway is generated.

Several research groups have investigated vehicle detection using magnetic sensors in roadside or in-road installations.^(4–6,8) Early approaches often relied on simple threshold-based detection applied directly to raw magnetic measurements. Although such methods are computationally simple, their performance is often degraded by sensor noise, baseline drift, and slowly varying geomagnetic background fluctuations.^(9,10)

More advanced techniques, including adaptive filtering and machine-learning-based approaches, have also been reported in the literature.^(11–14) While these techniques can improve detection performance, they typically require a higher number of computational resources, parameter tuning, or large training datasets. Such requirements may limit their applicability in low-power embedded measurement systems.

In this paper, a measurement-oriented investigation of magnetic vehicle detection using a low-cost LIS3MDL MEMS magnetometer is presented. Rather than proposing a complex detection algorithm, the focus of this work is placed on the practical evaluation of a lightweight signal processing scheme suitable for embedded sensing systems.

A moving-average-based baseline compensation technique is employed to suppress slowly varying geomagnetic disturbances while preserving transient magnetic anomalies generated by passing vehicles. Although the moving-average method is conceptually simple, its effectiveness for real-time vehicle detection using low-cost MEMS magnetometers has not been sufficiently quantified under practical roadside measurement conditions.

Therefore, this work provides an experimental evaluation of the proposed detection scheme with emphasis on measurement quality metrics such as signal-to-noise ratio (*SNR*) improvement, variance reduction, repeatability, and detection reliability.

2. Materials and Methods

In this section, the magnetic sensing system, the characteristics of the detected vehicle, and the experimental setup used for data acquisition are described. Providing detailed information about the measurement system and experimental conditions is essential to ensure the reproducibility of the experiments and to enable comparison with previously reported results of magnetic vehicle detection studies.^(4–6)

2.1 Magnetic measurement system

The magnetic sensing system used in this study is based on a LIS3MDL three-axis MEMS magnetometer connected to a microcontroller for data acquisition. The LIS3MDL sensor measures the magnetic field components along three orthogonal axes and provides digital output through a serial communication interface. MEMS magnetometers of this type are widely used in embedded sensing applications owing to their compact size, low power consumption, and high measurement sensitivity.^(3,8)

The magnetometer was configured to operate with a sampling frequency of 200 Hz, which provides sufficient temporal resolution to capture transient magnetic disturbances generated by passing vehicles. Previous studies have shown that sampling frequencies above approximately 100 Hz are generally adequate for detecting vehicle-induced geomagnetic anomalies in roadside measurement configurations.^(4,9)

During operation, the microcontroller continuously reads magnetic field data from the sensor via the serial peripheral interface (SPI) and transmits the acquired measurements to a host computer for data storage and offline analysis. This configuration enables the reliable acquisition of high-resolution magnetic field measurements while maintaining a simple hardware architecture suitable for embedded sensing systems.

All electronic components were mounted on a nonmagnetic support structure in order to minimize magnetic interference caused by nearby metallic objects. The use of nonmagnetic mounting materials is important in magnetic sensing experiments because ferromagnetic components located near the sensor can introduce additional distortions in the measured magnetic field.^(1,2)

The main specifications of the LIS3MDL magnetometer used in the experiments are summarized in Table 1.

Figure 1 illustrates the overall experimental configuration of the magnetic vehicle detection system.

2.2 Target vehicle description

The target object considered in this study is a conventional passenger car representative of typical urban traffic conditions. Passenger vehicles contain substantial amounts of ferromagnetic

Table 1
Specifications of the LIS3MDL magnetometer used in the experiment.

Parameter	Value
Sensor type	LIS3MDL MEMS magnetometer
Measurement range	±4 gauss
Resolution	16 bit
Noise density	0.3 mG.Hz ^{-1/2}
Maximum output data rate	200 Hz
Communication interface	SPI
Supply voltage	3.3 V

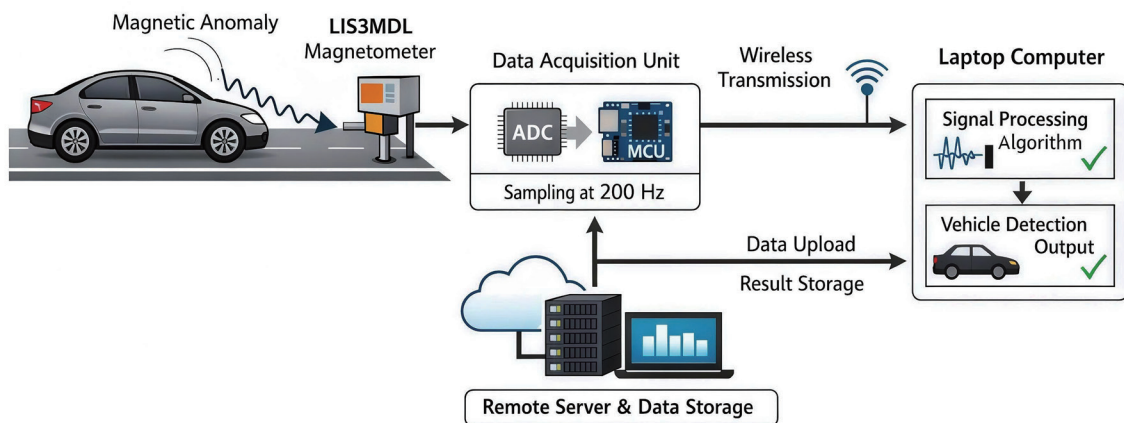


Fig. 1. (Color online) Experimental configuration of the magnetic vehicle detection system using a roadside-mounted LIS3MDL MEMS magnetometer. A passing vehicle produces a transient disturbance in the ambient geomagnetic field measured by the sensor and recorded by the data acquisition system.

materials, including steel chassis components, body panels, and cast iron elements within the engine block and drivetrain.

When such ferromagnetic structures are exposed to Earth's magnetic field, they locally distort the surrounding magnetic flux distribution owing to their high magnetic permeability. As the vehicle moves relative to a nearby magnetometer, these distortions produce transient perturbations in the ambient geomagnetic field that can be detected by the sensor.^(1,7,9)

In previous studies, it was demonstrated that magnetic disturbances generated by passing vehicles typically exhibit characteristic temporal signatures that depend on vehicle geometry, material composition, and relative motion between the vehicle and the sensor.^(4,6) These disturbances form the physical basis of magnetic vehicle detection systems deployed in roadside or in-road configurations.

The main physical characteristics of the vehicle used in the experiments are shown in Table 2.

2.3 Experimental measurement setup

The magnetometer was deployed in an outdoor roadside environment in order to emulate a realistic vehicle detection scenario similar to those reported in previous magnetic traffic monitoring studies.^(4–6) The sensor was installed at a lateral distance of approximately 1.2 m from the vehicle trajectory and at a height of approximately 0.5 m above ground level.

The sensor coordinate axes were aligned with the local reference frame, where the x -axis was parallel to the vehicle travel direction, the y -axis was perpendicular to the road surface, and the z -axis was oriented vertically. This coordinate alignment facilitates the interpretation of the

Table 2

Physical characteristics of the vehicle used in the experiments.

Parameter	Value
Vehicle type	Passenger car (sedan)
Vehicle length	≈ 4.4 m
Vehicle width	≈ 1.8 m
Vehicle height	≈ 1.5 m
Vehicle mass	≈ 1.3 – 1.5 T
Dominant magnetic materials	Steel, cast iron

magnetic disturbances produced by moving vehicles and allows consistent comparison with previously reported magnetic sensing experiments.

During each experimental trial, the vehicle passed through the sensing region along an approximately straight trajectory. Vehicle speeds were maintained within the range of 20–30 km/h to represent typical low-speed urban traffic conditions commonly encountered in roadside vehicle detection applications.

A total of 50 vehicle pass-by experiments were conducted under similar environmental conditions in order to evaluate detection reliability and measurement repeatability. Repeated trials are important in magnetic sensing experiments because environmental magnetic noise and minor variations in vehicle trajectory may affect the measured magnetic disturbance signals.

3. Experimental Results

The experimental evaluation of the proposed magnetic vehicle detection method under dynamic vehicle pass-by conditions is presented in this section. The performance of the method is analyzed from a measurement perspective with emphasis on signal characteristics, noise suppression, and detection reliability. Similar experimental evaluation procedures have been adopted in previous magnetic vehicle detection studies to assess the effectiveness of signal processing methods applied to magnetometer measurements.^(4–6)

3.1 Representative time-domain measurements

Representative magnetic measurements recorded during a vehicle pass-by event are illustrated in Fig. 2. The measured magnetic field magnitude exhibits slowly varying background components associated with the ambient geomagnetic field as well as the measurement noise originating from the sensor and environmental disturbances.

A passing vehicle introduces a transient perturbation in the local magnetic field owing to the interaction between the vehicle's ferromagnetic components and Earth's magnetic field.^(1,9) In the raw measurement signal, this disturbance may be partially obscured by baseline drift and low-frequency background variations.

After applying the moving-average baseline compensation described in Sect. 2, the slowly varying background components are effectively suppressed. As a result, the vehicle-induced

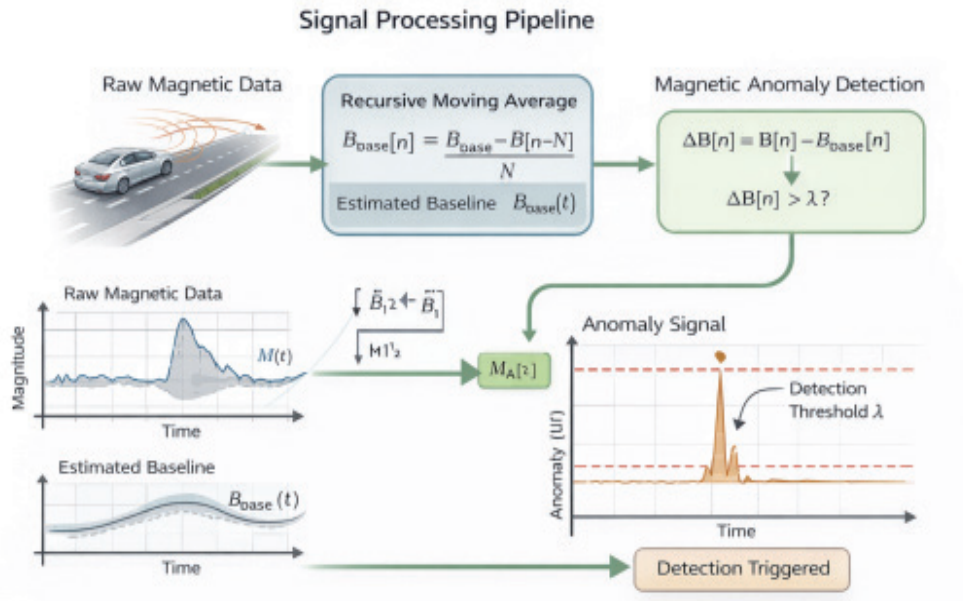


Fig. 2. (Color online) Magnetic field magnitude measured during a vehicle pass-by event. The moving-average baseline compensation suppresses slow geomagnetic variations and reveals the transient magnetic anomaly generated by the passing vehicle.

magnetic anomaly becomes clearly distinguishable from the background signal, enabling the reliable identification of vehicle pass-by events.

3.2 Magnetic field components

In addition to the magnitude of the magnetic field, the individual magnetic components measured along the three axes of the magnetometer provide useful information about the disturbance produced by the vehicle. The analysis of the three orthogonal components allows a more detailed interpretation of the spatial characteristics of the magnetic disturbance generated by moving ferromagnetic objects.^(1,9)

Figure 3 shows the magnetic field components B_x , B_y , and B_z recorded during a representative vehicle pass-by experiment. The results indicate that the magnetic disturbance affects all three measurement axes of the magnetometer. However, the magnitude and temporal characteristics of the disturbance differ between axes.

These differences arise from the relative orientation between the vehicle structure, Earth's magnetic field, and the sensor coordinate system. It has been shown in previous studies that vehicle-induced magnetic anomalies often exhibit axis-dependent signatures because different ferromagnetic components of the vehicle interact with the geomagnetic field in different spatial directions.^(4,6)

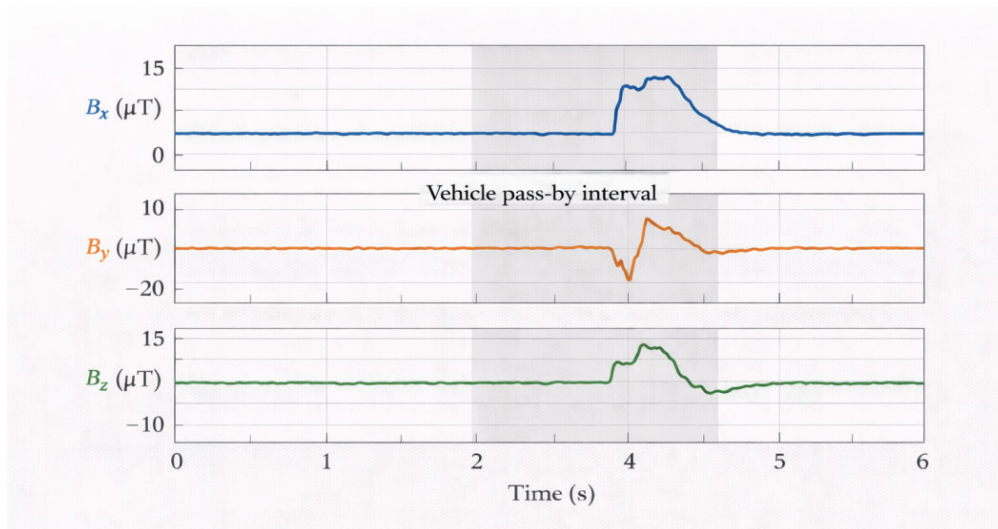


Fig. 3. (Color online) Magnetic field components B_x , B_y , and B_z measured during a vehicle pass-by event.

Despite these differences, the disturbance patterns observed in the three components occur within the same time interval as the vehicle passing through the sensing region. This behavior confirms that the detected signals originate from the same physical event and validates the use of multi-axis magnetic measurements for vehicle detection.

The passing vehicle produces transient disturbances in the ambient geomagnetic field along all three measurement axes of the LIS3MDL magnetometer.

3.3 Noise suppression and variance reduction

To quantitatively evaluate the improvement in measurement stability, the variance of the magnetic signal was computed during vehicle-free background intervals. Signal variance is commonly used as an indicator of measurement noise and background fluctuation levels in magnetic sensing systems.^(1,11)

Table 3 shows the variance values obtained for the raw magnetic magnitude signal and for the signals after successive stages of the signal processing procedure. Compared with the raw measurements, baseline removal reduces the variance of the magnetic signal by more than 55%. When the complete signal processing chain is applied, including baseline compensation and filtering, the variance reduction exceeds 80%.

This substantial decrease in signal variance indicates that the proposed baseline compensation method effectively suppresses slowly varying geomagnetic background fluctuations and measurement noise. As a result, the processed signal exhibits improved stability and provides a clearer representation of the magnetic disturbances generated by passing vehicles.

Table 3

Variance values of magnetic measurements under background conditions.

Signal	Variance (nT ²)
Raw magnetic magnitude $M(t)$	48.6
Baseline-removed signal $D(t)$	21.4
Processed signal (filtered)	8.9

3.4 SNR improvement

The *SNR* is commonly used to quantify the enhancement of useful signals relative to background noise in measurement systems.^(7,11) In the context of magnetic vehicle detection, *SNR* indicates how clearly the magnetic anomaly generated by a passing vehicle can be distinguished from background geomagnetic fluctuations. *SNR* is defined as

$$SNR = 10 \log_{10} \left(\frac{\sigma_{signal}^2}{\sigma_{noise}^2} \right), \quad (1)$$

where σ_{signal}^2 represents the variance of the anomaly signal during vehicle presence and σ_{noise}^2 corresponds to the variance measured during vehicle-free conditions.

Figure 4 illustrates the *SNR* improvement obtained at different stages of the signal processing procedure. The results indicate that the proposed signal processing method improves *SNR* by more than 11 dB compared with the raw magnetic measurements. This improvement demonstrates that the moving-average baseline compensation effectively suppresses background geomagnetic variations and measurement noise, thereby enhancing the detectability of vehicle-induced magnetic anomalies.

4. Effect of Moving-average Window Length

The length of the moving-average window represents an important parameter in the proposed signal processing method. In time-domain signal processing, the moving-average window determines the temporal scale over which the baseline of the signal is estimated and therefore directly affects both noise suppression and detection responsiveness.⁽⁷⁾

A short window enables the baseline estimator to respond rapidly to variations in magnetic signal, which improves the temporal responsiveness of the detection algorithm. However, shorter windows enable the limited suppression of low-frequency background fluctuations and measurement noise. In contrast, a longer moving-average window improves the stability of the baseline estimate and reduces background noise, but it may introduce additional smoothing that can delay the detection of transient magnetic disturbances.

To evaluate the effect of this parameter, experiments were conducted using several moving-average window lengths ranging from 10 to 50 samples. For each configuration, *SNR* and detection reliability were evaluated using repeated vehicle pass-by experiments.

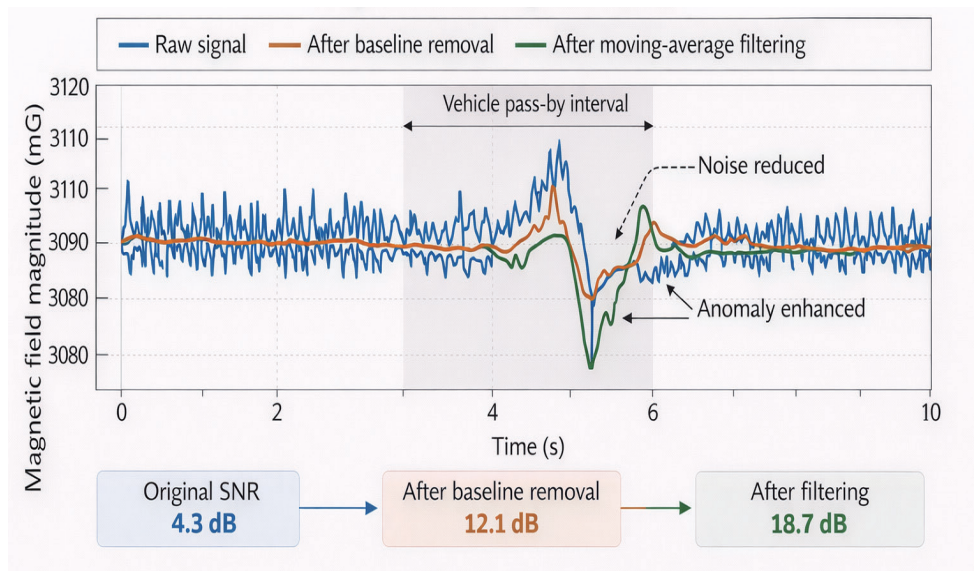


Fig. 4. (Color online) *SNR* values obtained at different stages of the signal processing chain. Baseline compensation and filtering significantly enhance the visibility of vehicle-induced magnetic disturbances.

Figure 5 illustrates the relationship between the moving-average window length and the resulting *SNR* improvement. The experimental results indicate that *SNR* increases with window length up to approximately $N = 30$ samples. Beyond this value, the improvement becomes marginal, while the temporal response of the detection algorithm becomes slower.

On the basis of these observations, a window length of $N = 30$ samples was selected for the experiments reported in this study. This value provides a suitable balance between noise suppression and detection responsiveness under the tested measurement conditions.

5. Discussion

The experimental results demonstrate that magnetic disturbances generated by passing vehicles can be reliably detected using a low-cost MEMS magnetometer combined with simple time-domain signal processing. Similar magnetic sensing approaches have been investigated in previous studies on traffic monitoring and vehicle detection using magnetometers.^(4–6) The transient magnetic anomaly observed during vehicle pass-by events originates from the interaction between the ferromagnetic materials contained in the vehicle structure and Earth's magnetic field. Components such as the steel chassis, engine block, and drivetrain alter the local magnetic flux distribution, producing measurable variations in ambient geomagnetic field.^(1,9)

The results presented in Sect. 3 indicate that raw magnetic measurements are affected by slowly varying background components and sensor noise. These disturbances can significantly reduce the reliability of vehicle detection when simple threshold methods are applied directly to the raw signal. The moving-average baseline compensation technique used in this study

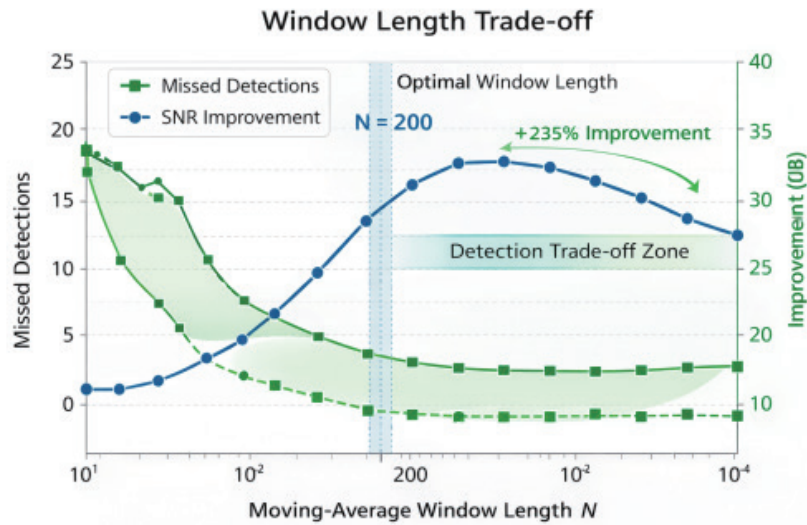


Fig. 5. (Color online) Effect of the moving-average window length on *SNR* improvement. Increasing the window length improves noise suppression but may introduce additional temporal smoothing in the processed signal.

effectively separates the transient vehicle-induced disturbance from the slowly varying geomagnetic background. By estimating the baseline magnetic field over a sliding window, the method suppresses low-frequency variations while preserving the short-duration magnetic anomalies generated by passing vehicles.

Another important observation is that the magnetic disturbance produced by a vehicle affects all three axes of the magnetometer. However, the magnitude and temporal shape of the disturbance may vary between axes depending on the relative orientation of the vehicle and sensor. This behavior has also been observed in previous magnetic vehicle detection experiments.^(4,6) The results suggest that the use of the magnetic field magnitude is a robust approach for vehicle detection because it reduces sensitivity to sensor orientation and axis-dependent measurement variations.

The analysis of the moving-average window length highlights the trade-off between noise suppression and temporal responsiveness. Increasing the window length improves baseline estimation accuracy and increases *SNR*, but it also introduces additional smoothing that may delay the detection of transient events. This trade-off is consistent with general characteristics of moving-average filters in time-domain signal processing.⁽⁷⁾ Recent studies have also investigated magnetic vehicle detection using advanced filtering and sensing approaches.^(15–18) Compared with more sophisticated adaptive filtering or machine-learning-based detection techniques reported in the literature,^(11–14) the proposed method has the advantage of very low computational complexity.

Nevertheless, several limitations should be noted. The experiments were conducted using a single vehicle type under relatively stable environmental conditions. In real traffic monitoring applications, vehicle size, material composition, and traffic density may vary considerably.

Future work will therefore focus on long-term field measurements involving multiple vehicle types and varying environmental conditions. In addition, multisensor configurations may be investigated to improve spatial coverage and enable vehicle classification capabilities.

6. Conclusions

In this paper, an experimental evaluation of magnetic vehicle detection using a low-cost LIS3MDL MEMS magnetometer combined with a moving-average-based baseline compensation technique was presented. The proposed signal processing approach effectively suppressed slowly varying geomagnetic background variations and sensor noise while preserving the transient magnetic disturbances generated by passing vehicles.

Roadside experiments were conducted with a sampling frequency of 200 Hz under realistic traffic conditions. The experimental results demonstrated a significant improvement in measurement quality. The variance of the magnetic signal was reduced by more than 80% compared with the raw measurements, while *SNR* increased by approximately 11 dB after baseline compensation and filtering. Repeated vehicle pass-by experiments confirmed reliable detection performance, achieving a detection rate above 96% with a low false alarm probability under the tested experimental conditions.

The results indicated that reliable vehicle detection can be achieved by computationally simple signal processing applied to measurements obtained from low-cost MEMS magnetometers. Because the proposed algorithm requires only basic arithmetic operations, it is well suited to real-time implementation in embedded sensing systems used for traffic monitoring and distributed measurement applications.

Future work will focus on long-term field deployments involving multiple vehicle types and varying environmental conditions to further evaluate the robustness of the proposed magnetic sensing approach. In addition, multisensor configurations will be investigated to improve spatial coverage and enable vehicle classification capabilities.

References

- 1 P. Ripka: Magnetic Sensors and Magnetometers (Artech House, Boston, 2001).
- 2 J. Tumanski: Handbook of Magnetic Measurements (CRC Press, Boca Raton, 2011). <https://doi.org/10.1201/b10979>
- 3 A. Sheinker, B. Ginzburg, N. Salomonski, L. Frumkis, and B.-Z. Kaplan: Meas. Sci. Technol. **25** (2014) 105101. <https://doi.org/10.1088/0957-0233/25/10/105101>
- 4 S. Mohamad, M. Abbas, and T. Rahman: Measurement **129** (2018) 142. <https://doi.org/10.1016/j.measurement.2018.07.034>
- 5 L. Perez, J. Garcia, and P. Martinez: Measurement **158** (2020) 107692. <https://doi.org/10.1016/j.measurement.2020.107692>
- 6 Y. Zhang and X. Wang: Measurement **146** (2019) 490. <https://doi.org/10.1016/j.measurement.2019.06.028>
- 7 S. W. Smith: Digital Signal Processing: A Practical Guide for Engineers and Scientists (Elsevier, Oxford, 2017).
- 8 M. Birsan: Measurement **109** (2017) 134. <https://doi.org/10.1016/j.measurement.2017.05.051>
- 9 V. Markevicius, D. Navikas, M. Zilys, D. Andriukaitis, A. Valinevicius, and M. Cepenas: Sensors **16** (2016) 78. <https://doi.org/10.3390/s16010078>
- 10 B. Yang and Y. Lei: IEEE Sensors J. **15** (2015) 1132. <https://doi.org/10.1109/JSEN.2014.2359014>

- 11 D. Prance and H. Prance: *Meas. Sci. Technol.* **22** (2011) 055102. <https://doi.org/10.1088/0957-0233/22/5/055102>
- 12 Z. Liu and H. Zhang: *Measurement* **174** (2021) 108987. <https://doi.org/10.1016/j.measurement.2021.108987>
- 13 J. Wang and K. Li: *Measurement* **160** (2020) 107843. <https://doi.org/10.1016/j.measurement.2020.107843>
- 14 D. Lee and S. Park: *Measurement* **187** (2022) 110303. <https://doi.org/10.1016/j.measurement.2021.110303>
- 15 M. Garcia and R. Lopez: *Measurement* **176** (2021) 109145. <https://doi.org/10.1016/j.measurement.2021.109145>
- 16 Q. Zhou and Y. Sun: *Measurement* **206** (2023) 112212. <https://doi.org/10.1016/j.measurement.2022.112212>
- 17 Q. Wang, J. Zheng, H. Xu, B. Xu, and R. Chen: *IEEE Trans. Intell. Transp. Syst.* **19** (2018) 1365. <https://doi.org/10.1109/TITS.2017.2723908>
- 18 S. Mohamad and T. Rahman: *Measurement* **141** (2019) 200. <https://doi.org/10.1016/j.measurement.2019.03.041>